Bull. Chem. Soc. Ethiop. **2023**, 37(1), 47-58.
DOI: https://dx.doi.org/10.4314/bcse.v37i1.5

ISSN 1011-3924
Printed in Ethiopia
Online ISSN 1726-801X

INVESTIGATION OF ADSORPTION OF BASIC ORANGE 2 DYE ON MONTMORILLONITE AND ERROR ANALYSIS

Baybars Ali Fil*

Balıkesir University, Engineering Faculty, Department of Environmental Engineering, 10145-Çağış/Balıkesir, Turkey

(Received April 19, 2022; Revised August 22, 2022; Accepted August 23, 2022)

ABSTRACT. In this study, isotherm studies were investigated for the removal of basic orange 2 (BO2) dye on the montmorillonite surface. Two-parameter isotherm models such as Langmir, Freundlich, and Temkin isotherms and Three-parameter isotherm models such as Sips, Toth, and Khan isotherms were calculated by non-linear analysis method. The adsorption capacity at equilibrium was calculated by adding 0.035 g of adsorbent at 10-300 mg/L concentrations to 100 mL of synthetic dyestuff solution at room temperature. According to the results obtained, it was determined that the isotherm data matched the Langmuir isotherm with a regression coefficient of 0.995 from the Two-parameter models, and the Sips isotherm with a regression coefficient of 0.998 from the Three-parameter isotherm models. In addition, according to the results of error analysis, it was determined that the lowest error value fit the HYBRID model. SNE values support the HYBRID model.

KEY WORDS: Adsorption, Basic orange 2, Isotherm models; Error analyses, Hybrid

INTRODUCTION

As a result of the rapid progress of industrialization, it has triggered population growth in certain regions. Growing industries and increasing population have also led to the consumption of clean water resources faster than they should have been. Therefore, the protection of clean water resources is a growing problem day by day [1]. The textile industry is one of the leading industries that need a clean water source. The amount of clean water used during dyeing varies according to the type of fabric and yarn, but reaches enormous amounts [2]. In addition, depending on the processes of the textile product, the wastewater may contain color, COD, flow, turbidity, and toxic substances [3].

Due to this, either inadequate treatment of wastewater from the textile industry before it was released into receiving settings, or inadequate treatment followed by sophisticated treatment methods before the treated water was released back into the system. Thus, either the pollution of the environment is prevented or the consumption of clean water resources can be prevented by reclaiming the water [4].

Many methods have been described in the literature for the treatment of textile industry wastewater. These include biological treatment [5, 6], membrane filtration [7, 8], adsorption [9-11], coagulation-flocculation [12], chemical oxidation [13], electrofenton [14], and electrooxidation [15].

Adsorption, often known as adhesion, is a chemical and physical force that affects how dissolved solids, liquids, and gases adhere to surfaces through their atoms. It has an adhesive force of some sort. On easily graspable surfaces, adsorption forms a holding strip. The "adsorption" force and sticky absorption are distinct in this regard. Fluids can permeate and dissolve solids and liquids, respectively, via adsorption. Adsorption is a phenomenon and phenomenon connected to the adhesive force of surfaces, whereas absorption is related to the densities of materials. Many materials can be used as adsorbent in the adsorption process.

*Corresponding author. E-mail: baybarsalifil2@gmail.com

Among these methods, adsorption is highly preferred in textile wastewater treatment when a suitable and effective adsorbent is used. Activated carbon [16, 17], biosorbent [18, 19], montmorillonite [20], bentonite [21, 22], sepiolite [23], illite [24], zeolite [25], kaolin [26], clay [17] can be listed as the main adsorbent types.

While the isotherm parameters can be found using linear and/or nonlinear regression techniques, the applicability of the isotherm models can be assessed using correlation coefficient (R^2) and/or error analysis [27]. The isotherm equation is set up linearly for the linear regression method. The adsorption data are plotted after that. The slope and intercept of the plot can be used to determine the isotherm parameters. An error function is necessary in the case of the nonlinear regression technique. By minimizing the difference between the computed and experimental data, the isotherm parameters can be found. However, in some instances, it was discovered that the parameters computed using the linear regression approach were distinct from those derived using the nonlinear regression method [28]. Additionally, because each of the error functions has generated its own set of parameters, the nonlinear regression approach might provide several sets of isotherm parameters.

In this study, 2/1 type montmorillonite clay with high surface area was used. Equilibrium isotherms of basic orange 2 (BO2) dyestuff were investigated in synthetically prepared wastewater. For equilibrium isotherm studies, two-parameter (Langmuir, Freundlich, and Temkin) and three-parameter (Toth, Sips and Khan) isotherm models were applied to the experimental data. Compatible isotherm models and related coefficients were calculated from the obtained results. In addition, their optimizations were evaluated using various error analyzes given.

EXPERIMENTAL

Supply of adsorbents and formation of the solution

From Süd-Chemie, montmorillonite clay samples were acquired (Turkey). The physical characteristics and chemical makeup of montmorillonite have been described in earlier research [29]. The dye was acquired from Sigma-Aldrich Company and utilized without additional purification (Germany). Basic Orange 2 (BO2), **I**, has a molecular weight of 248.72 g/mol and the chemical formula $C_{12}H_{12}N_4HCl$ [30]. Orcozine chrysoidine 4 is another name for this color. A certain quantity of dye was dissolved in distilled water at a concentration of 1000 mg/L to create the stock solution. To create the experimental solutions, distilled water was used to dilute a stock solution of BO2 to the required concentration.

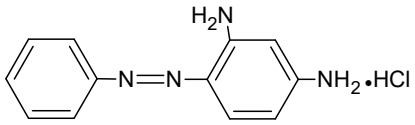

I (molecular structure of Basic Orange 2)

Investigations and experimental computations

The influences of experimental parameters of pH, agitation speed, ionic strength, adsorbent dosage, contact time, and initial dye concentration on the adsorptive removal of BO2 were studied in a batch mode. In each adsorption experiment, the 100 mL samples of BO2 solution with known concentration was put in a 250 mL Erlenmeyer flask, and then the varying amount of adsorbent was added into the flask. All experiments were carried out at the fixed (293 K) temperature. The pH of the dye solution was adjusted by using 0.01 M HCl and 0.01 M NaOH. The agitation speeds

of 100–400 rpm were studied for the effect of the agitation on adsorption experiments. The ionic strength of the aqueous solutions was adjusted with NaCl for experiments. The adsorbent was separated from solution by centrifugation at 10000 rpm for 10 min. The concentration of dye in samples was determined during adsorption experiments by using UV-Visible spectrophotometer (Spekol-1100) at 455 nm wavelength absorption for BO2. The calibration straight line ($R^2 = 0.99$) was obtained in the ranges 1–15 mg/L.

The adsorption capacity was calculated using the following equation:

$$q_e = \left(\frac{C_0 - C_e}{m} \right) \times V \tag{1}$$

where C_0 and C_e were initial and equilibrium concentrations of BO2 (mg/L), respectively, m was the mass of adsorbent (g) and V was volume of the solution (L).

Adsorption isotherm models

The adsorption isotherm is very important to establish the most appropriate correlation for the equilibrium data in adsorption batch system. The adsorption isotherm study was performed at 10, 25, 50, 75, 100, 125, 150, 175, 200, 225, 250, and 300 mg/L initial dye concentration at 293 K temperature, pH 4.25 (natural), 0.35 g/L amount of adsorbent, and 300 rpm agitation speed. The compatibility of the equilibrium data obtained from the adsorption experiments is evaluated with the Langmuir [31], Freundlich [32], Temkin [33], Toth [34], Sips [35], and Khan [36] isotherm models. The mathematical equations for these isotherm models and kinetic models are given in Table 1.

Table 1. Mathematical equations of isotherm models.

Isotherm model	Mathematical equation	Eq. no.	Ref.
Langmuir	$q_e = \frac{q_m \cdot K_L \cdot C_e}{1 + K_L \cdot C_e}$	(2)	[31]
Freundlich	$q_e = K_F \cdot C_e^{1/n}$	(3)	[32]
Temkin	$q_e = \left(\frac{R \cdot T}{b} \right) \cdot \ln \left(K_T \cdot C_e \right)$	(4)	[33]
Toth	$q_e = \frac{q_m \cdot C_e}{\left(K_{To} + \mathrm{C}_e^n \right)^{1/\mathrm{n}}}$	(5)	[34]
Sips	$q_e = \frac{q_m \cdot \mathrm{a_S} \cdot \mathrm{C}_e^{1/n}}{1 + \mathrm{a_S} \cdot \mathrm{C}_e^{1/n}}$	(6)	[35]
Khan	$q_e = \frac{q_\mathrm{m} \cdot b_K \cdot C_e}{\left(1 + b_K \cdot \mathrm{C_e} \right)^{a_K}}$	(7)	[36]

Error analysis

The isotherm parameters have been found using the original forms of isotherm equations because of the inherent bias caused by linearization. Therefore, the isotherm equations are solved without linearization. In the isotherm studies, the optimization process requires an error function to be defined in order to be able to determine the fit of the isotherm to the experimental data. In the

current work, five different error functions were studied and in each case, the isotherm parameters were determined by minimizing the respective error function across the concentration range studied using the solver add-in with Microsoft's spreadsheet. The error functions studied were detailed in the follows.

The sum of squares of errors

The sum of the squares of the errors (SSE) is one of the most commonly used functions among error functions:

$$SSE = \sum_{i=1}^{n} \left(q_{calc} - q_{meas} \right)_i^2 \tag{8}$$

The major trouble is that the size of the errors, thereby the square of the errors increases as the concentration gets higher. Isotherm parameters provide a better fit toward the adsorption obtained at the higher values of concentration [37]. Where q_{meas} represents the results obtained from the experimental data and q_{calc} represents the values obtained as a result of the error analysis.

The hybrid fractional error function

The hybrid fractional error function (HYBRID) provides better fit, especially at low concentrations compared to SSE:

$$HYBRID = \frac{100}{n-p} \sum_{i=1}^{n} \left[\frac{\left(q_{cal} - q_{meas} \right)^2}{q_{meas}} \right]_i \tag{9}$$

The square of each error value is divided by the experimental equilibrium adsorption values. The equation also includes the degree of freedom of the system, for example, the number of data points, n, minus the number of parameters, p, of the isotherm equation [38].

Average relative error

The average relative error (ARE) is intended to minimize the fractional error distribution across all concentration range. The number of experiments is included as a divisor of the equation [39].

$$ARE = \frac{100}{n} \sum_{i=1}^{n} \left| \frac{q_{cal} - q_{meas}}{q_{meas}} \right|_i \tag{10}$$

Marquardt's percent standard deviation

Marquardt's percent standard deviation (MPSD) [40] was studied by a number of researchers in the field [41]. It is similar in some respects to a geometric mean error distribution modified according to the number of degrees of freedom of the system [37].

$$MPSD = 100 \sqrt{\frac{1}{n-p} \sum_{i=1}^{n} \left(\frac{q_{cal} - q_{meas}}{q_{meas}} \right)_i^2} \tag{11}$$

The sum of the absolute errors

The sum of the absolute errors (SAE) is similar to the sum of the squares of the errors. Isotherm parameters calculated using this error function will provide a better fit when the size of the errors increase, biasing the fit towards the high concentration data [38].

$$SAE = \sum_{i=1}^{n} \left| q_{calc} - q_{meas} \right|_i \tag{12}$$

Optimization of error functions

Linear regression and nonlinear regression performance for the estimation of adsorption isotherm parameters can be evaluated using the procedure of normalizing and combining error results to determine the "sum of normalized errors, SNE"[42]. The SNE values for each parameter set are then compared. The most suitable result is accepted from the method that provides the lowest SNE value. The parameter values thus providing the least normalized error sum can be considered to be optimal for that isotherm provided." [43]

RESULTS AND DISCUSSION

Adsorption isotherm models and error analysis

The "SNE" was taken into account to select the optimum isotherm parameter set. With this calculation method, each parameter set is tested for all error functions to give error values for each error function. The resulting error values were divided by the maximum errors for that error function and the results for each error function were combined as the SNE value. The parameter set giving the smallest SNE value was accepted as the optimum parameter set [44].

Due to the inherent bias from linearization, alternative single-component parameter sets were determined by nonlinear regression using five different error functions previously described, namely SSE, HYBRID, ARE, MPSD, and SAE. Minimizing the respective error functions over the experimental concentration ranges yielded the isotherm constants (Table 2-7). Application of different error functions will yield different sets of isotherm constants that are sometimes close to each other and therefore difficult to compare [45].

For all the isotherm models examined, the smallest SNE values in all data sets were obtained with the HYBRID error function [46]. When all the tables in which the results are given are examined, the relevant regression coefficients also support these inferences (Tables 2-7). In nonlinear regression analysis, Langmuir isotherm equation gave the best fit with experimental data among two parameter isotherm models. In the three parameter isotherm models, although the R^2 values are close to each other, the Sips isotherm is seen as the most compatible isotherm.

As shown in these tables, the results tend to suggest that a lower absolute error value is obtained for both the Langmuir and Sips isotherms. There is good agreement between the experimental value and the calculated value. Based on the R^2 values, the best order of fit was obtained as Sips > Langmuir > Khan > Toth > Temkin > Freundlich according to the nonlinear analysis.

Table 2. Non-linear error analysis of isotherm models for the adsorption of BO2 onto montmorillonite for Langmuir isotherm.

	SSE	SAE	ARE	HYBRID	MPSD
q_m	398.047	402.011	402.079	394.185	402.045
K_L	0.129	0.115	0.115	0.136	0.115
R^2	0.994	0.993	0.993	0.995	0.993
SSE	972.801	939.041	933.287	**932.447**	932.681
SAE	78.411	72.708	72.764	**71.267**	72.721
ARE	6.046	5.548	**5.546**	6.506	5.547
HYBRID	96.212	99.805	98.144	**92.467**	98.061
MPSD	**11.389**	12.461	12.474	11.498	12.470
SNE	4.806	4.744	4.723	**4.716**	4.721

Table 3. Non-linear error analysis of isotherm models for the adsorption of BO2 onto montmorillonite for Freundlich isotherm.

	SSE	SAE	ARE	HYBRID	MPSD
K_F	107.513	108.791	65.846	72.243	66.028
n	3.674	3.739	2.502	2.743	2.506
R^2	0.852	0.910	0.788	0.911	0.790
SSE	1528.295	**1515.819**	1728.178	1613.038	1742.750
SAE	367.153	**364.500**	377.757	367.896	376.246
ARE	33.781	34.281	23.618	24.747	**23.598**
HYBRID	1341.609	1424.779	1446.804	**1290.178**	1443.816
MPSD	44.946	46.613	45.846	45.338	**39.746**
SNE	4.726	4.819	4.664	**4.486**	4.535

Table 4. Non-linear error analysis of isotherm models for the adsorption of BO2 onto montmorillonite for Temkin isotherm.

	SSE	SAE	ARE	HYBRID	MPSD
b	35.758	33.869	34.032	35.124	33.983
K_T	2.472	2.197	2.200	2.286	2.199
R^2	0.984	0.979	0.980	0.985	0.981
SSE	2718.854	2695.329	**2448.712**	2481.984	2516.845
SAE	152.554	**151.339**	151.449	152.160	151.416
ARE	6.322	4.738	4.737	5.192	**4.735**
HYBRID	91.559	93.779	96.791	**89.091**	98.715
MPSD	7.577	6.502	6.345	**6.119**	6.389
SNE	4.928	4.541	4.461	**4.442**	4.510

Table 5.Non-linear error analysis of isotherm models for the adsorption of BO 2 onto montmorillonite for Khan isotherm.

	SSE	SAE	ARE	HYBRID	MPSD
q_m	355.432	337.199	336.902	339.331	324.250
b_K	0.157	0.164	0.173	0.170	1.523
a_K	0.964	0.933	0.924	0.950	0.960
R^2	0.991	0.912	0.938	0.996	0.976
SSE	874.601	860.311	894.895	891.058	**846.545**
SAE	85.762	86.039	84.127	**82.454**	89.826
ARE	6.396	6.636	6.753	**6.132**	6.621
HYBRID	93.109	96.596	97.345	**91.839**	95.808
MPSD	12.290	**12.279**	12.319	12.707	12.321
SNE	4.803	4.860	4.906	**4.765**	4.880

Table 6. Non-linear error analysis of isotherm models for the adsorption of BO2 onto montmorillonite for Sips isotherm.

	SSE	SAE	ARE	HYBRID	MPSD
q_m	399.253	400.159	400.929	405.611	400.929
a_S	0.145	0.159	0.109	0.141	0.109
n	1.056	1.066	0.977	1.069	0.977
R^2	0.996	0.995	0.993	0.998	0.992
SSE	528.796	540.568	528.147	**523.214**	530.139
SAE	75.332	75.818	**73.757**	75.417	77.757
ARE	6.765	6.556	6.359	6.229	**6.003**
HYBRID	94.817	100.064	97.357	**92.653**	97.698
MPSD	13.650	17.590	14.166	**13.563**	14.460
SNE	4.671	4.944	4.644	**4.556**	4.666

Table 7. Non-linear error analysis of isotherm models for the adsorption of BO2 onto montmorillonite for Toth isotherm.

	SSE	SAE	ARE	HYBRID	MPSD
q_m	418.276	400.899	373.906	413.384	373.906
K_{To}	4.458	5.874	4.501	5.079	5.523
n	0.819	1.005	1.048	0.858	1.084
R^2	0.993	0.992	0.980	0.994	0.979
SSE	692.913	729.492	692.597	712.445	**690.823**
SAE	78.265	78.727	**76.670**	77.587	78.519
ARE	6.690	**5.242**	5.494	6.456	5.995
HYBRID	51.561	58.563	55.635	**50.609**	52.502
MPSD	14.685	14.319	14.793	**13.347**	14.330
SNE	4.817	4.752	4.695	**4.694**	4.706

The graphical representation of the results based on the HYBRID error analysis also clearly demonstrates the compatibility between the experimental data and the isotherm models. The comparison of the two parameter isotherm models with the experimental results in Figure 1 shows that the Langmuir isotherm model is the most compatible isotherm model. Comparison of three parameter isotherm models with experimental data is shown in Figure 2. It is clearly seen from the figure that the best fit between the experimental data and the studied isotherm models is the Sips isotherm model. Figure 3 shows the comparison of the Langmuir isotherm model, one of the two parameter isotherm models, and the Sips isotherm model, one of the 3-parameter isotherm models, with the experimental results.

This shows that the size of the error function alone should not be considered when choosing the optimum isotherm. Instead, when choosing the optimum isotherm, both the size of the error function and the determined isotherm parameters should be verified against the theory behind the isotherm.

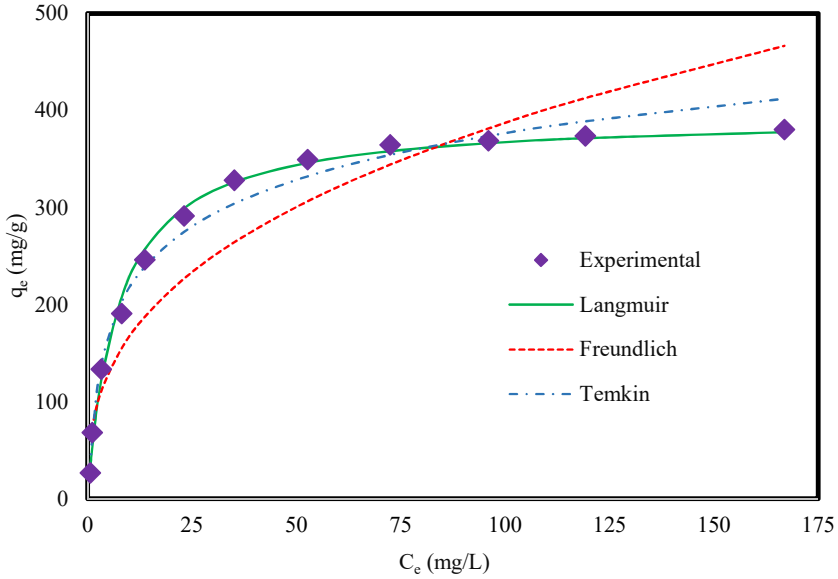

Figure 1. Comparison of two parameter isotherm models based on HYBRID analysis.

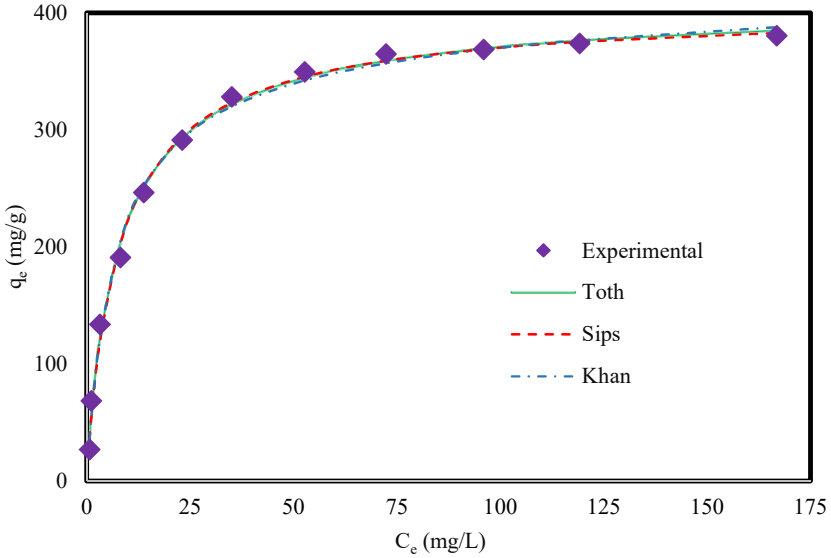

Figure 2. Comparison of three parameter isotherm models based on HYBRID analysis.

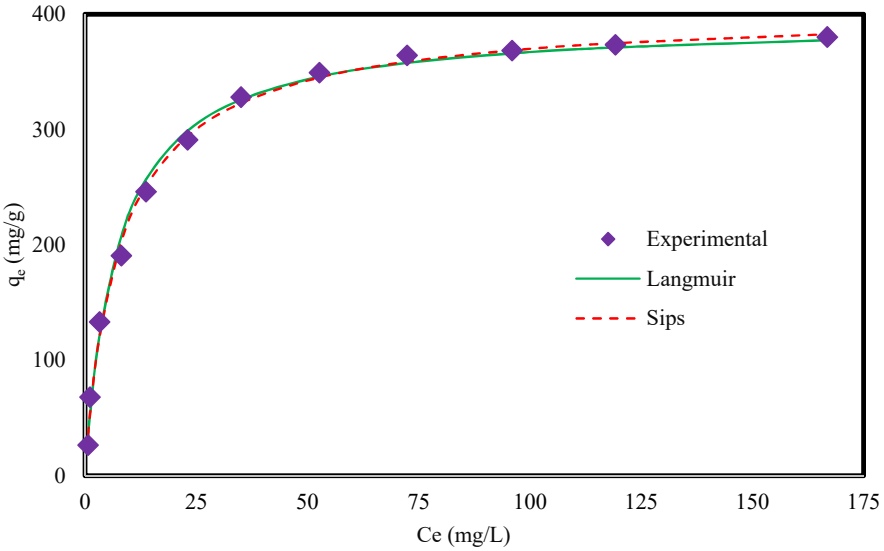

Figure 3. Comparison of the most compatible isotherm models on the basis of HYBRID analysis.

CONCLUSION

This study shows that montmorillonite clays can efficiently remove BO2 from aqueous solutions. In addition, It was determined that Langmuir isotherm was the most compatible isotherm model among the two-parameter isotherm models. It was concluded that the most compatible isotherm model among the three-parameter isotherm models is the Sips isotherm. When all isotherm models are compared, it was discussed that there would be an order such as Sips > Langmuir > Khan > Toth > Temkin > Freundlich. Error function analysis among the 6 adsorption systems found that HYBRID error function provided the best overall results. Sips performs the best prediction as it is the best fit model determined using HYBRID method with the experimental data.

ACKNOWLEDGEMENTS

The authors are grateful for financial support of Balikesir University Scientific Research Project Department (Project No: 2022/053)

REFERENCES

1. Foo, K.Y.; Hameed, B.H. Utilization of biodiesel waste as a renewable resource for activated carbon: Application to environmental problems. *Renew. Sust. Energ. Rev.* **2009**, 13, 2495-2504.
2. Lellis, B.; Fávaro-Polonio, C.Z.; Pamphile, J.A.; Polonio, J.C. Effects of textile dyes on health and the environment and bioremediation potential of living organisms. *Biotechnol. Res. Innovation* **2019**, 3, 275-290.
3. Holkar, C.R.; Jadhav, A.J.; Pinjari, D.V.; Mahamuni, N.M.; Pandit, A.B. A critical review on textile wastewater treatments: Possible approaches. *J. Environ. Manage.* **2016**, 182, 351-366.

4. Naik, D.J.; Desai, H.; Desai, T.N. Characterization and treatment of untreated wastewater generated from dyes and dye intermediates manufacturing industries of Sachin Industrial Area, Gujarat, India. *J. Environ. Res. Develop.* **2013**, 7, 1602-1605.
5. Singare, P.U. Fluidized aerobic bio-reactor technology in treatment of textile effluent. *J. Environ. Chem. Eng.* **2019**, 7, 102899.
6. Dhanve, R.S.; Shedbalkar, U.U.; Jadhav, J.P. Biodegradation of diazo reactive dye Navy blue HE2R (Reactive blue 172) by an isolated Exiguobacterium sp. RD3. *Biotechnol. Bioprocess Eng.* **2008**, 13, 53-60.
7. Marszałek, J.; Żyłła, R. Recovery of water from textile dyeing using membrane filtration processes. *Processes* **2021**, 9, 1833.
8. Fersi, C.; Gzara, L.; Dhahbi, M. Treatment of textile effluents by membrane technologies. *Desalination* **2005**, 185, 399-409.
9. Wong, S.; Ghafar, N.A.; Ngadi, N.; Razmi, F.A.; Inuwa, I.M.; Mat, R.; Amin, N.A.S. Effective removal of anionic textile dyes using adsorbent synthesized from coffee waste. *Sci. Rep.* **2020**, 10, 2928.
10. Kaur, S.; Rani, S.; Mahajan, R.K. Adsorption kinetics for the removal of hazardous dye congo red by biowaste materials as adsorbents. *J. Chem.* **2013**, 2013, 628582.
11. Khodaie, M.; Ghasemi, N.; Moradi, B.; Rahimi, M. Removal of methylene blue from wastewater by adsorption onto $ZnCl_2$ activated corn husk carbon equilibrium studies. *J. Chem.* **2013**, 2013, 383985.
12. Liang, Z.; Wang, Y.; Zhou, Y.; Liu, H. Coagulation removal of melanoidins from biologically treated molasses wastewater using ferric chloride. *Chem. Eng. J.* **2009**, 152, 88-94.
13. Azbar, N.; Yonar, T.; Kestioglu, K. Comparison of various advanced oxidation processes and chemical treatment methods for COD and color removal from a polyester and acetate fiber dyeing effluent. *Chemosphere* **2004**, 55, 35-43.
14. Malakootian, M.; Moridi, A. Efficiency of electro-Fenton process in removing Acid Red 18 dye from aqueous solutions. *Process Saf. Environ. Prot.* **2017**, 111, 138-147.
15. Yavuz, Y.; Savaş Koparal, A.; Öğütveren, Ü.B. Electrochemical oxidation of Basic Blue 3 dye using a diamond anode: evaluation of colour, COD and toxicity removal. *J. Chem. Technol. Biotechnol.* **2011**, 86, 261-265.
16. Djilani, C.; Zaghdoudi, R.; Djazi, F.; Bouchekima, B.; Lallam, A.; Modarressi, A.; Rogalski, M. Adsorption of dyes on activated carbon prepared from apricot stones and commercial activated carbon. *J. Taiwan Inst. Chem. Eng.* **2015**, 53, 112-121.
17. Bendaho, D.; Driss, T.A.; Bassou, D. Adsorption of acid dye onto activated Algerian clay. *Bull. Chem. Soc. Ethiop.* **2017**, 31, 51-62.
18. Silva, F.; Nascimento, L.; Brito, M.; da Silva, K.; Paschoal, W., Jr.; Fujiyama, R. Biosorption of Methylene Blue Dye Using Natural Biosorbents Made from Weeds. *Materials* **2019**, 12, 2486.
19. Tesfaw, B.; Chekol, F.; Mehretie, S.; Admassie, S. Adsorption of Pb(II) ions from aqueous solution using lignin from Hagenia abyssinica. *Bull. Chem. Soc. Ethiop.* **2016**, 30, 473-484.
20. Khaniabadi, Y.O.; Basiri, H.; Nourmoradi, H.; Mohammadi, M.J.; Yari, A.R.; Sadeghi, S.; Amrane, A. Adsorption of congo red dye from aqueous solutions by montmorillonite as a low-cost adsorbent. *Int. J. Chem. React. Eng.* **2018,** 16, 20160203.
21. Zhu, X.; Lan, L.; Xiang, N.; Liu, W.; Zhao, Q.; Li, H. Thermodynamic studies on the adsorption of Cu^{2+}, Ni^{2+} and Cd^{2+} on to amine-modified bentonite. *Bull. Chem. Soc. Ethiop.* **2016**, 30, 354-367.
22. Unuabonah, E.I.; Olu-Owolabi, B.I.; Böhm, L.; Düring, R.A. Adsorption of polynuclear aromatic hydrocarbons from aqueous solution: Agrowaste-modified kaolinite vs surfactant modified bentonite. *Bull. Chem. Soc. Ethiop.* **2016**, 30, 369-376.

23. Yu, J.; Zou, A.; He, W.; Liu, B. Adsorption of mixed dye system with cetyltrimethyl ammonium bromide modified sepiolite: Characterization, performance, kinetics and thermodynamics. *Water* **2020**, 12, 981.
24. Omer, O.S.; Hussein, B.H.M.; Ouf, A.M.; Hussein, M.A.; Mgaidi, A. An organified mixture of illite-kaolinite for the removal of Congo red from wastewater. *J. Taibah Univ. Sci.* **2018**, 12, 858-866.
25. Thongkam, M.; Trisupakitti, S.; Palama, T.; Senajuk, W.; Nausri, C. Adsorption kinetic of direct dyes from aqueous solution on zeolite LTA. *Sci. Technol. Asia* **2021**, 26, 1-8.
26. Dias, M.; Valério, A.; de Oliveira, D.; Ulson de Souza, A.A.; de Souza, S.M.G.U. Adsorption of natural annatto dye by kaolin: Kinetic and equilibrium. *Environ. Technol.* **2020**, 41, 2648-2656.
27. Gimbert, F.; Morin-Crini, N.; Renault, F.; Badot, P.-M.; Crini, G. Adsorption isotherm models for dye removal by cationized starch-based material in a single component system: Error analysis. *J. Hazard. Mater.* **2008**, 157, 34-46.
28. Slimani, R.; El Ouahabi, I.; Abidi, F.; El Haddad, M.; Regti, A.; Laamari, M.R.; Antri, S.E.; Lazar, S. Calcined eggshells as a new biosorbent to remove basic dye from aqueous solutions: Thermodynamics, kinetics, isotherms and error analysis. *J. Taiwan Inst. Chem. Eng.* **2014**, 45, 1578-1587.
29. Fil, B.A.; Özmetin, C.; Korkmaz, M. Characterization and electrokinetic properties of montmorillonite. *Bulg. Chem. Commun.* **2014**, 46, 258-263.
30 Silva Martínez, S.; Vergara Sánchez, J.; Moreno Estrada, J.R.; Flores Velásquez, R. FeIII supported on ceria as effective catalyst for the heterogeneous photo-oxidation of basic orange 2 in aqueous solution with sunlight. *Sol. Energy Mater Sol. Cells* **2011**, 95, 2010-2017.
31. Langmuir, I. The adsorption of gases on plane surfaces of glass, mica and platinum. *J. Am. Chem. Soc.* **1918**, 40, 1361-1403.
32. Freundlich, H. Over the adsorption in solution. *J. Phys. Chem.* **1906**, 57, 385-470.
33. Temkin, M.I. Adsorption equilibrium and the kinetics of processes on nonhomogeneous surfaces and in the interaction between adsorbed molecules. *Zh. Fiz. Chim.* **1941**, 15, 296-332.
34. Tóth, J. Calculation of the BET-compatible surface area from any type I isotherms measured above the critical temperature. *J. Colloid Interface Sci.* **2000**, 225, 378-383.
35. Sips, R. On the structure of a catalyst surface. *J. Chem. Phys.* **1948**, 16, 490-495.
36. Khan, A.R.; Al-Waheab, I.R.; Al-Haddad, A. A Generalized equation for adsorption isotherms for multi-component organic pollutants in dilute aqueous solution. *Environ. Technol.* **1996**, 17, 13-23.
37. Chan, L.; Cheung, W.; Allen, S.; McKay, G. Error analysis of adsorption isotherm models for acid dyes onto bamboo derived activated carbon. *Chin. J. Chem. Eng.* **2012**, 20, 535-542.
38. Porter, J.F.; McKay, G.; Choy, K.H. The prediction of sorption from a binary mixture of acidic dyes using single- and mixed-isotherm variants of the ideal adsorbed solute theory. *Chem. Eng. Sci.* **1999**, 54, 5863-5885.
39. Kapoor, A.; Yang, R.T. Correlation of equilibrium adsorption data of condensible vapours on porous adsorbents. *Gas Separ. Purif.* **1989**, 3, 187-192.
40. Marquardt, D.W. An algorithm for least-squares estimation of nonlinear parameters. *J. Soc. Indust. Appl. Math.* **1963**, 11, 431-441.
41. Seidel, A.; Gelbin, D. On applying the ideal adsorbed solution theory to multicomponent adsorption equilibria of dissolved organic components on activated carbon. *Chem. Eng. Sci.* **1988**, 43, 79-88.
42. Ho, Y.; Porter, J.; McKay, G. Equilibrium isotherm studies for the sorption of divalent metal ions onto peat: copper, nickel and lead single component systems. *Water Air Soil Pollut.* **2002**, 141, 1-33.

43. Prasad, A.L.; Santhi, T.; Manonmani, S. Recent developments in preparation of activated carbons by microwave: Study of residual errors. *Arabian J. Chem.* **2015**, 8, 343-354.
44. Shahmohammadi-Kalalagh, S.; Babazadeh, H. Isotherms for the sorption of zinc and copper onto kaolinite: comparison of various error functions. *Int. J. Environ. Sci. Technol.* **2014**, 11, 111-118.
45. Vasanth Kumar, K.; Sivanesan, S. Sorption isotherm for safranin onto rice husk: Comparison of linear and non-linear methods. *Dyes Pigm.* **2007**, 72, 130-133.
46. Chan, L.S.; Cheung, W.H.; Allen, S.J.; McKay, G. Error analysis of adsorption isotherm models for acid dyes onto bamboo derived activated carbon. *Chin. J. Chem. Eng.* **2012**, 20, 535-542.